Autocrine CXCL12 regulates the proliferation of glioma stem cells

著者	上前 洋二
year	2014
その他のタイトル	CXCL12のオートクリンはグリオーマ幹細胞の増殖を制御する
学位授与大学	筑波大学 (University of Tsukuba)
学位授与年度	2014
報告番号	12102甲第7085号
URL	http://hdl.handle.net/2241/00126569

筑　波　大　学

博 士 （医 学） 学 位 論 文

CXCL12 secreted from glioma stem cells regulates their proliferation

（グリオーマ幹細胞から分泌される CXCL12 は、
自身の増殖を制御する）

２０１４

筑波大学大学院博士課程人間総合科学研究科
上前　洋二

CONTENTS

Abstract

Background: Emerging evidence suggests that the chemokine CXCL12 and its receptor CXCR4, which are expressed by glioma stem cells (GSCs), play an important role in tumorigenesis. To provide evidence for establishing a new therapy targeting the CXCL12/CXCR4 pathway, we investigated whether CXCL12 secreted from GSCs contributed to their proliferation and promoted angiogenesis in murine GSCs.

Methods: Angiogenetic functions and proliferation of GSCs with or without CXCL12 inhibitors were evaluated in an in vitro model using tube formation assays, RT-PCR, and proliferation, as well as in an in vivo syngenic model.

Results: In endothelial culture, the morphology and gene expression of GSCs changed from stem cell-like characteristics to endothelial cell-like features. CXCL12 expression increased in endothelial cell-like GSCs. CXCL12 blockage with siRNA or shRNA markedly inhibited cell proliferation in vitro. CXCL12 knockdown with shRNA also inhibited tumor growth in vivo. On the other hand, CXCL12/CXCR4 blockage affected neither tube formation in vitro nor angiogenesis in vivo.

Conclusions: The CXCL12 secreted from GSCs (autocrine/paracrine CXCL12) regulates their proliferation, but probably not angiogenesis.

The final publication is available at link.springer.com

http://link.springer.com/article/10.1007%2Fs11060-014-1364-y

Introduction

High-grade gliomas are the most common primary brain tumors in adults and include World Health Organization (WHO) grade III anaplastic glioma and WHO grade IV glioblastoma multiforme (GBM). GBM is an intractable disease, characterized by high proliferation of tumor cells and intense angiogenesis. The standard therapy is maximal surgical tumor removal, followed by focal radiotherapy and chemotherapy with temozolomide, resulting in a median overall survival not exceeding 2 years [1]. Various therapies, including endovascular-targeting therapy and tumor-specific antigen-targeting therapy, have been developed for the treatment of patients with high-grade gliomas [2-5]. Glioma stem cells (GSCs) express some features that are resistant to chemotherapy and radiation therapy. These cells promote tumor angiogenesis by interacting with tumor-associated endothelial cells [6] and by secreting high levels of vascular endothelial growth factor (VEGF) [7]. Interestingly, a significant portion of endothelial cells in GBM originates from tumor-derived cells [8, 9]. We have studied the molecular mechanisms of glioma angiogenesis and glioma-associated endothelial biology using human glioblastoma samples [10]. On the other hand, two independent phase III clinical trials for GBM with bevacizumab, RTOG-0825, and AVAGlio showed that anti-VEGF therapy in GBM significantly prolongs progression-free survival, but does not improve overall survival [11]. These results raise the issue of how important anti-angiogenesis therapy is in GBM.

Chemokines were originally identified as a family of molecules that regulate the chemotaxis of leukocytes. In the field of cancer, CXC chemokine ligand 12 (CXCL12/SDF-1) and its receptor, CXCR4, also regulate tumorigenesis in breast, lung, prostate, and pancreatic cancers [12-15]. In brain tumors, CXCR4 is expressed by a subpopulation of glioblastoma cells with stem cell properties [16]. In contrast, the other receptor, CXCR7, is exclusively expressed by the bulk of the more differentiated glioblastoma cells as well as most of the established glioblastoma cell lines [17]. A previous study showed that

the binding of CXCL12 to CXCR4 induces intracellular signaling through ERK1/2 or PI3K [18]. The CXCL12/CXCR4 signaling pathway promotes tumorigenesis of GSCs [16, 19, 20] and angiogenesis by inducing VEGF [7]. The function of CXCL12 in GSCs has been analyzed in detail in very few reports. One previous report showed that invasive glioma cells significantly overexpress CXCR4 and CXCL12 compared to noninvasive glioma cells [21].

To better understand the role of CXCL12 in GSC biology, we have now performed an integrated study in which we simultaneously evaluated the contribution of the CXCL12/CXCR4 signaling pathway to proliferation and angiogenesis using murine GSCs.

Materials and Methods

Cell lines and mice

A syngenic murine GSC cell line, called the tumor sphere cell line (TS), was established by Dr. Hideyuki Saya (Division of Gene Regulation, Keio University School of Medicine, Tokyo, Japan) [22, 23]. The TS cell was established by overexpressing H-Ras^{V12} in normal neural stem/progenitor cells isolated from the subventricular zone of adult mice harboring a homozygous deletion of the *Ink4a/Arf* locus. All mice after TS cell implantation developed highly invasive, hypervascular glioblastoma-like tumors, which was green fluorescent protein (GFP)$^{+}$, nestin^{+} and CD44^{+} cell. [23] TS cells were cultured in neural stem cell medium (NSM), which consisted of Dulbecco's modified Eagle medium (DMEM)/F12 (Sigma, St. Louis, MO) supplemented with 20 ng/ml epidermal growth factor (PeproTech, Rocky Hill, NJ), 20 ng/ml basic fibroblast growth factor (PeproTech), B27 supplement without vitamin A (Invitrogen, Carlsbad, CA), 200 ng/ml heparan sulfate, 100 U/ml penicillin, and 100 ng/ml streptomycin. The cells were also cultured in endothelial cell medium (ECM), which consisted of HuMeda-EG2 (Kurabo, Osaka, Japan) supplemented with 100 U/ml penicillin and 100 ng/ml streptomycin. In all experiments, tumor spheres were dissociated to obtain a single-cell suspension before use. A syngenic murine glioma cell line, GL261, was obtained from Dr. Masahiro Toda (Department of Neurosurgery, Keio University School of Medicine, Tokyo, Japan) and maintained in Minimal eagle medium (MEM) supplemented with 10% fetal calf serum (FCS) and 1% penicillin-streptomycin solution (Sigma). The F-2 murine vascular endothelial cell line was derived from a murine (BALB/c × C57BL/6) subcutaneous tumor and transformed using ultraviolet radiation. These cells were provided by Riken BioResource Center Cell Bank (Tsukuba, Ibaraki) and cultured in DMEM (Gibco®; Life Technologies Corp., Carlsbad, CA) with 10% FCS and 1% penicillin-streptomycin. At each passage, cells were harvested as single-cell suspensions using trypsin/ethylenediaminetetra-acetic acid.

Cells were incubated in a humidified atmosphere containing 5% CO_2 at 37°C.

Male C57BL/6 mice aged 6 weeks were purchased from Clea Japan, Inc. (Tokyo). The mice were maintained under constant temperature and humidity in a light-controlled environment with free access to food and water. All animal experiments in this study followed the guidelines for animal experimentation of the ethics committee of the Laboratory Animal Resource Center in the University of Tsukuba.

RNA preparation and RT-PCR

Total RNA was extracted using RNeasy (QIAGEN, Venlo, Netherlands) according to the manufacturer's protocol. Reverse transcription was performed with 3.68 μg total RNA from each sample in a total volume of 20 μl using the PrimeScript II 1st strand cDNA Synthesis Kit (TaKaRa Bio Inc., Ohtsu, Shiga, Japan) according to the manufacturer's protocol.

The sequences of the forward and reverse primers are as follows: VEGFA-Fw 5′-TTCAGAGCGGAGAAAGCATT-3′, VEGFA-Rev 5′-GAGGAGGCTCCTTCCTGC-3′, CXCL12-Fw 5′-GAAGTGGAGCCATAGTAATGCC-3′, CXCL12-Rev 5′-TCCAAGTGGAAAAATACACCG-3′, CXCR4-Fw 5′-TTCTCATCCTGGCCTTCATC-3′, CXCR4-Rev 5′-CTTTTCAGCCAGCAGTTTCC-3′, CXCR7-Fw 5′-GCCGTACCATTTTGTGGTTC-3′, CXCR7-Rev 5′-TGCAACGCTGTAAAGAGCAC-3′, β-actin-Fw 5′-GAAGTGTGACGTTGACAT-3′, β-actin-Rev 5′-ACATCTGCTGCTGGAAGGTG-3′. β-actin was used as a loading control. PCR was performed using TAKARA Ex Taq (TaKaRa) according to the manufacturer's protocol. The reaction mixture contained 1 μl forward primer (10 μM) and 1 μl reverse primer (10 μM) in a final volume of 25 μl. PCR was performed as follows: 94°C for 5 min; 35 cycles of 94°C for 30 sec, annealing temperature (listed in Table 1) for 90 sec, and 72°C for 60 sec. The PCR products were separated on a 2% agarose gel, visualized with ethidium bromide staining, and

photographed with FAS-III Series (NIPPON Genetics Co., Ltd., Tokyo, Japan).

Molecular design of gene targets and gene knock down using siRNAs and shRNA

For siRNA transfection, the designed four pairs of siRNAs (duplexes of sense and anti-sense strands) were synthesized by Invitrogen (Valencia, CA). These siRNAs were 25-nucleotide-long double-stranded RNA oligos. In our experiments to suppress CXCL12 expression in TS cells, we used the most effective siRNAs among them (targeted sequences of CXCL12 were sense 5′-CCAGAGCCAACGUCAAGCAUCUGAA-3′ and antisense 5′-UUCAGAUGCUUGACGUUGGCUCUGG-3′). Stealth RNAi negative control with Medium GC Duplex (Invitrogen) was used as a negative control. Transient transfection of synthetic siRNA was achieved using Lipofectamine 2000 transfection reagent (Invitrogen). In brief, 1×10^5 cells were plated in 6-cm culture dishes. Lipofectamine 2000 was diluted in Opti-MEM I medium without serum and incubated for 5 min. CXCL12 siRNA or negative control siRNA was each diluted in Opti-MEM I medium without serum and added to the diluted Lipofectamine 2000. The mixture was incubated for 20 min at room temperature to allow the siRNA or negative control siRNA:Lipofectamine 2000 complexes to form. A 500-µl aliquot of complexes was added to each dish, and cells were incubated for another 72 h without replacing the medium.

For shRNA transfection, the designed shRNAs were synthesized by OriGene (Rockville, MD). The targeted sequence of CXCL12 was sense 5′-CCTGCCGGTTCTTCGAGAGCCACATCGCC-3′. An ineffective 29-mer scrambled shRNA cassette in the pRS Vector (OriGene) was used as a negative control. Transfection was performed the same way as for siRNA. Stable cell lines were prepared in medium containing 10 µg/ml puromycin.

Quantitative real-time RT-PCR, cell proliferation assays, tube formation assay, and ELISA

We used the MiniOpticon Real-Time PCR Detection System (Bio-Rad, Hercules, CA) for real-time PCR using iQ^{TM} SYBR Green Supermix (Bio-Rad). Relative quantification of PCR products was calculated after normalization to β-actin.

For cell proliferation assays, CXCL12 siRNAs or control siRNAs were transfected into TS cells with Lipofectamine 2000 (Invitrogen). TS cells were incubated with 2 ml of culture medium ± drug per dish at 37°C for 72 h. At the end of the incubation, the cell number was quantified using a hemocytometer after staining with crystal violet.

For the tube formation assay, 1×10^5 cells were incubated in 300 μl growth factor-reduced Matrigel (Becton Dickinson and Company, Franklin Lakes, NJ) in a 4-well multi-dish (Thermo Fisher Scientific, Waltham, MA) at 37°C in a 5% CO_2 incubator. The Matrigel wells were digitized under a 4× objective lens (KEYENCE, Osaka, Japan).

For ELISA, TS cells were plated at 1.25×10^6 cells/ml, cell culture supernatants were collected after 24 h of culture, and VEGF concentrations were measured using Quantikine ELISA Kits (R&D Systems, Minneapolis, MN). All standards and samples were assayed in duplicate. All assays were performed according to the protocols recommended by the manufacturers.

Injection of TS cells into C57BL/6 Mice

As a subcutaneous tumor mouse model, TS cells transfected with control shRNA or CXCL12 shRNA were injected subcutaneously (1×10^5 cells/100 μl) into the back area of C57BL/6 mice, and tumor burden was observed for up to 4 weeks. The size of the tumors was measured three times per week with calipers. Tumor volume (*TV*) was calculated using the formula: $TV = W^2 * L/2$ (where *W* is the shortest diameter, and *L* is the longest diameter). Four weeks after implantation, mice were sacrificed by cervical

spine dislocation under anesthesia.

As an intracranial tumor mouse model, C57BL/6 mice were placed in a stereotactic frame (SR-5M with IMS-3 microinjector; Narishige, Tokyo, Japan) under anesthesia with isoflurane (induction 4%; maintenance 2%). The striatum was targeted unilaterally in the right hemisphere using a 27-G needle (Hamilton) connected to a Hamilton 100-µl syringe. The stereotactic coordinates for the microinjections were: 0.5 mm anterior, 2.5 mm lateral to bregma. TS cells transfected with control shRNA or CXCL12 shRNA were injected intracranially (1×10^5 cells/10 µl) over a period of 3 min. Mice were sacrificed after 2 weeks.

Histological analysis including Immunohistochemistry (IHC)

For IHC, frozen tumor tissue samples were fixed with zinc fixative for 24 h, embedded in OTC compound, and cut into 5-µm sections with a cryostat. After washing the slides twice in distilled water, they were incubated with rabbit polyclonal anti-CXCL12 antibodies (Santa Cruz Biotechnology, Inc., Dallas, TX; 1:50), rabbit monoclonal anti-von willebrand factor (vWF) antibodies (Dako Denmark A/S, Glostrup, Denmark; 1:200), or rat monoclonal anti-F4/80 antibodies (AbD Serotec, Oxford, UK; 1:100) for 1 h at room temperature. Subsequently, sections were rinsed twice with phosphate-buffered saline (PBS) and incubated with anti-rabbit Alexa Fluor 555 antibody (Life Technologies Corp.) or anti-rat Alexa Fluor 594 antibody (Life Technologies Corp.) for 30 min at room temperature followed by washing with PBS for 10 min. The sections were then incubated in DAPI for 2 min followed by washing with PBS for 5 min. The positive area (pixels/view) was measured using morphometry software (KEYENCE).

Prior to CD31 staining, sections were incubated with 0.3% hydrogen peroxide in methanol for 20 min to inhibit endogenous peroxidases. Sections were incubated with rat monoclonal anti-CD31 antibodies

(Becton Dickinson and Company; 1:10) for 1 h at room temperature. Binding of the primary antibodies was detected using anti-rat biotinylated antibody (Dako) and the LSAB 2 streptavidin–biotin horseradish peroxidase kit (Dako). Antibody complexes were then visualized by incubation with diaminobenzidine chromogen (Lab Vision kit). Sections were counterstained with Mayer's hematoxylin.

Statistical analysis

The data are presented as the mean ± standard error. Statistically significant differences between the groups were determined with the Student's two-tailed t-test and/or Tukey's honestly significant difference (HSD) test. All p-values were 2-sided; values were considered statistically significant at $p < 0.05$.

Results

The morphology and gene expression of TS cells changed from stem cell-like to endothelial cell-like in endothelial cell medium

Previously, we demonstrated that glioma-derived endothelial cells are genetically and functionally distinct from normal endothelial cells [10]. In addition, a subpopulation of GSCs is able to differentiate into functional endothelial cells [8, 9]. Thus, to examine the angiogenic potential of TS cells in vitro, we analyzed the molecular, morphological, and expression changes in NSM or ECM. TS cells formed floating neurospheres in NSM, whereas the cells changed to adherent cells in ECM. TS cells in NSM did not form tube-like structures on Matrigel. After pre-incubation for 10 days in ECM, TS cells formed tube-like structures on Matrigel. In contrast, GL261 cells did not form tube-like structures regardless of pre-incubation (Figure 1A, B). TS cells in ECM consisted of adherent and floating cells. We analyzed each type of TS cells separately. Only the adherent type formed tube-like structures (Figure 1C). Thus, adherent GSCs in ECM acquired the ability to form tube-like structures.

To analyze the molecular biological effects due to differences in culture conditions, we performed RT-PCR for endothelial cell-associated molecules. VEGF and CXCL12 expression in TS cells in ECM was higher than expression in TS cells in NSM. CXCR4 was expressed only in TS cells, and the expression was not affected by the type of medium (Figure 2A). When we separately analyzed expression in the adhesive type and the floating type of cells in ECM, the adherent cells expressed higher levels of VEGF and CXCL12 than the floating cells (Figure 2B). The adhesive TS cells acquired CXCL12 expression at the same time as the tube-like morphological change in ECM.

CXCL12 regulates the proliferation of GSCs in vitro

To evaluate the functional role of CXCL12 activity in TS cells, we used AMD3100 (CXCR4

antagonist) for inhibition of proliferation. Treatment with AMD3100 significantly reduced proliferation in a concentration-dependent manner (Figure 3A). For direct evidence of the importance of CXCL12 secreted from GSCs, CXCL12 siRNA was used to silence endogenous CXCL12 mRNA. CXCL12 siRNA efficiently reduced CXCL12 mRNA expression in TS cells, and transfection of the siRNA into TS cells resulted in 63% inhibition of the cell proliferation compared to control siRNA transfection (Figure 3B). We next performed CXCL12 shRNA knockdown using another sequence of CXCL12. Cells were transfected with lipofectamine and CXCL12 shRNA or control shRNA, and stable cell lines were established using puromycin selection. Similar to the CXCL12 siRNA knockdown results, we observed that CXCL12 shRNA in TS cells significantly reduced CXCL12 mRNA expression and attenuated cell growth in vitro (Figure 3C).

CXCL12/CXCR4 inhibitors do not affect formation of tube-like structures

To evaluate whether formation of the tube-like structures depends on CXCL12/CXCR4 signaling, AMD3100 or CXCL12 shRNA in TS cells was used in the tube formation assay. Inhibition of CXCL12/CXCR4 did not affect tube formation (Figure 4A). Figure 4B shows that VEGF production was up-regulated by fetal bovine serum but was not affected by CXCL12 and AMD3100. These in vitro data indicate that the functions of TS cells that are related to angiogenesis were independent of CXCL12/CXCR4 signaling.

CXCL12 silencing directly inhibits tumor growth in an in vivo model

We investigated the growth properties of GSCs in vivo after autocrine CXCL12 knockdown. Subcutaneous transplantation models of TS cells transfected with control shRNA or CXCL12 shRNA were used. Quantification of tumor size showed that CXCL12 knockdown in TS cells resulted in

significantly smaller tumors than control cells (Figure 5A). CXCL12 expression in glioma tissues from TS cells was observed using IHC. TS cells with CXCL12 shRNA tended to be lower than that from TS cells with control shRNA (Figure 5B). To determine whether the inhibition effect was associated with angiogenesis in the glioma tissue, the numbers of vessels in the glioma tissues obtained from intracranial TS cell transplantation and subcutaneous transplantation were calculated. As shown in Figure 5C, IHC using a vWF antibody and CD31 antibody showed that TS cells led to development of tumor vessels regardless of CXCL12 shRNA both in the subcutaneous and intracranial tumor models, suggesting that CXCL12 silencing directly inhibited glioma growth independent of angiogenesis.

GFP^+ cells (TS cells) were included among the $CD31^+$ endothelial cells (Figure 5D), demonstrating TS cells were differentiated into endothelial cells. We did not detect a difference in angiogenesis regardless of CXCL12 reduction. To analyze the reason, we performed IHC with anti-F4/80 antibody to label macrophages/ microglias, which typically promote angiogenesis. We found that many $F4/80^+$ cells had infiltrated into the tumor, regardless of CXCL12 (Figure 5E).

Discussion

Previous studies have not clarified whether CXCL12/CXCR4 signal blockage inhibits GSC growth as a direct effect of the signal blockage or as an indirect effect through blocking angiogenesis. In addition, the importance of another effect due to differentiation of GSCs into endothelial cells should be considered. Thus, we assessed the direct and indirect effects.

First, regarding the direct effect of CXCL12 on the GSCs themselves, we hypothesized that CXCL12 secreted from GSCs would induce cell proliferation through CXCR4 activation. In the present study, we showed that CXCL12 blockage inhibited tumor growth using murine GSCs both in vitro and in vivo. In addition, GSCs expressed CXCL12 mRNA (Figure 2 and 3) and CXCL12 protein (Figure5B). A previous paper showed that CXCL12 and CXCR4 associate to enhance proliferation and migration of glioma cells [24].

Our data showed that endothelial-like differentiation of GSCs was associated with CXCL12 expression (Figure1 and 2). Our previous experiments have shown that glioblastoma-derived endothelial cells exhibit a phenotype of activated endothelial cells, as reflected in the high expression of VEGF, CXCL12, and CXCR7 [10]. Another previous study reported that endothelial cells interact closely with brain cancer stem cells and that their interactions accelerate initiation and tumor growth to maintain perivascular stem cell niches [25]. Because GSC recruitment to the perivascular niche depends on the CXCL12/CXCR4 pathway, we propose that high CXCL12 expression by endothelial-like GSCs enhances the interaction between GSCs and tumor vessels. Recent animal studies have suggested that CXCL12 mediates apoptosis resistance to chemotherapy in glioma cells [26, 27]. These results indicate that CXCL12 provided by endothelial-like GSCs may be an important target for therapeutic approaches. The role of endothelial-like GSCs may be to create a particular environment for GSCs rather than to directly facilitate growth.

Second, regarding the indirect effect of host-derived endothelial cells, another study reported that CXCR4 promotes GSC-mediated VEGF production and tumor angiogenesis [7]. Several studies have reported that GSCs promote angiogenesis via VEGF [28, 29]. VEGF is an important molecule in tumor vessel formation, and VEGF neutralizing antibodies block tube formation [30]. However, CXCL12 did not alter VEGF production in our study (Figure 4B). CXCL12/CXCR4 signal blockage in GSCs significantly inhibited tumor growth without affecting angiogenesis (Figure 4A, 5A, C). We cannot explain this discrepancy between our study using a murine syngenic model and the result from another study regarding CXCR4 promotion and VEGF production using primary human tumor-derived xenograft models [7]. Therefore, further studies will be needed using other GSC models.

Considering our results, GSCs may activate angiogenesis independent of CXCL12/CXCR4 signaling. A possibility is that GSCs may increase the accumulation of host macrophages/microglias and endothelial progenitor cells independent of CXCL12/CXCR4 signaling. Indeed, we performed a preliminary analysis of the infiltration of macrophages/microglias in GSC tissues with IHC using anti-mouse F4/80 antibody. Regardless of CXCL12 knockdown, many macrophages/microglias infiltrated into GSCs tissues (Figure 5E). These cells may secrete large amount of VEGF and other molecules in tumor tissue. Further studies will be needed to access the reason of the accumulation of host macrophages/microglias. And a further limitation, our study did not assess the interactions between CXCL12/CXCR4 signaling and cell-cycle/cell-death-related molecules or other regulatory proteins including ubiquitin, which is also a natural ligand of CXCR4 [31]. Such evaluations using our model should be planned in the future..

In conclusion, CXCL12 blockage markedly inhibited GSC growth in vitro and in vivo. These results indicate that CXCL12 secreted from GSCs is a key system for glioma tumorigenesis. In contrast, the effect of CXCL12 blockage against angiogenesis is limited.

Acknowledgments

First of all I would like to thank my academic supervisor, Professor Akira Matsumura, who gave me the opportunity to carry out my research, for his guidance, support and supervision.

I would also like to thank my advisor Dr. Eiichi Ishikawa for his advice, guidance and practical comments on my research and dissertation. He was always eager to help and gave me valuable advice at each stage of my research. Without his support, comments and supervision I would not have been able to finish this study and prepare this thesis work.

I would particularly like to acknowledge Dr. Satoru Osuka, Dr. Masahide Matsuda, Dr. Noriaki Sakamoto, Dr. Shingo Takano, Dr. Kei Nakai and Dr. Tetsuya Yamamoto for their valuable help and advice on my study.

I also thank Professor Hideyuki Saya, as he kindly provided the Tumor Sphere cell line (TS).

And finally, I would like to thank my family and my colleagues in the Department of Neurosurgery, Faculty of Medicine, University of Tsukuba, without whom I could not have completed my study.

This study was supported by Grants-in-Aid for Scientific Research from the Japan Society for the Promotion of Science (No. 30510169 to EI).

References

1) Stupp R, Mason WP, van den Bent MJ, Weller M, Fisher B, Taphoorn MJ, Belanger K, Brandes AA, Marosi C, Bogdahn U, Curschmann J, Janzer RC, Ludwin SK, Gorlia T, Allgeier A, Lacombe D, Cairncross JG, Eisenhauer E, Mirimanoff RO; European Organisation for Research and Treatment of Cancer Brain Tumor and Radiotherapy Groups; National Cancer Institute of Canada Clinical Trials Group (2005) Radiotherapy plus concomitant and adjuvant temozolomide for glioblastoma. N Engl J Med 352:987-996.

2) Ishikawa E, Tsuboi K, Takano S, Uchimura E, Nose T, Ohno T (2004) Intratumoral injection of IL-2-activated NK cells enhances the antitumor effect of intradermally injected paraformaldehyde-fixed tumor vaccine in a rat intracranial brain tumor model. Cancer Sci 95:98-103.

3) Ishikawa E, Tsuboi K, Yamamoto T, Muroi A, Takano S, Enomoto T, Matsumura A, Ohno T (2007) Clinical trial of autologous formalin-fixed tumor vaccine for glioblastoma multiforme patients. Cancer Sci 98:1226-1233.

4) Muragaki Y, Maruyama T, Iseki H, Tanaka M, Shinohara C, Takakura K, Tsuboi K, Yamamoto T, Matsumura A, Matsutani M, Karasawa K, Shimada K, Yamaguchi K, Nakazato Y, Sato K, Uemae Y, Ohno T, Okada Y, Hori T (2011) Phase I/IIa trial of autologous formalin-fixed tumor vaccine concomitant with fractionated radiotherapy for newly diagnosed glioblastoma. J Neurosurg 115:248-255

5) Okaji Y, Tsuno NH, Tanaka M, Yoneyama S, Matsuhashi M, Kitayama J, Saito S, Nagura Y, Tsuchiya T, Yamada J, Tanaka J, Yoshikawa N, Nishikawa T, Shuno Y, Todo T, Saito N, Takahashi K, Nagawa H (2008) Pilot study of anti-angiogenic vaccine using fixed whole endothelium in patients with progressive malignancy after failure of conventional therapy. Eur J Cancer 44:383-390

6) Folkins C, Shaked Y, Man S, Tang T, Lee CR, Zhu Z, Hoffman RM, Kerbel RS (2009) Glioma tumor stem-like cells promote tumor angiogenesis and vasculogenesis via vascular endothelial growth factor and stromal-derived factor 1. Cancer Res 69:7243-7251

7) Ping YF, Yao XH, Jiang JY, Zhao LT, Yu SC, Jiang T, Lin MC, Chen JH, Wang B, Zhang R, Cui YH, Qian C, Wang J, Bian XW (2011) The chemokine CXCL12 and its receptor CXCR4 promote glioma stem cell-mediated VEGF production and tumour angiogenesis via PI3K/AKT signalling. J Pathol 224:344-54

8) Ricci-Vitiani L, Pallini R, Biffoni M, Todaro M, Invernici G, Cenci T, Maira G, Parati EA, Stassi G, Larocca LM, De Maria R (2010) Tumour vascularization via endothelial differentiation of glioblastoma stem-like cells. Nature 468:824-828

9) Soda Y, Marumoto T, Friedmann-Morvinski D, Soda M, Liu F, Michiue H, Pastorino S, Yang M, Hoffman RM, Kesari S, Verma IM (2011) Transdifferentiation of glioblastoma cells into vascular endothelial cells. Proc Natl Acad Sci U S A 108:4274-4280

10) Takano S, Yamashita T, Ohneda O (2010) Molecular therapeutic targets for glioma angiogenesis. J Oncol 2010:351908

11) Weller M, Yung WK (2013) Angiogenesis inhibition for glioblastoma at the edge: beyond AVAGlio and RTOG 0825. Neuro Oncol 15:971

12) Koshiba T, Hosotani R, Miyamoto Y, Ida J, Tsuji S, Nakajima S, Kawaguchi M, Kobayashi H, Doi R, Hori T, Fujii N, Imamura M (2000) Expression of stromal cell-derived factor 1 and CXCR4 ligand receptor system in pancreatic cancer: a possible role for tumor progression. Clin Cancer Res 6:3530-3535

13) Müller A, Homey B, Soto H, Ge N, Catron D, Buchanan ME, McClanahan T, Murphy E, Yuan W, Wagner SN, Barrera JL, Mohar A, Verástegui E, Zlotnik A (2001) Involvement of chemokine

receptors in breast cancer metastasis. Nature 410:50-56

14) Sun YX, Wang J, Shelburne CE, Lopatin DE, Chinnaiyan AM, Rubin MA, Pienta KJ, Taichman RS (2003) Expression of CXCR4 and CXCL12 (SDF-1) in human prostate cancers (PCa) in vivo. J Cell Biochem 89:462-473

15) Wald O, Shapira OM, Izhar U (2013) CXCR4/CXCL12 axis in non small cell lung cancer (NSCLC) pathologic roles and therapeutic potential. Theranostics 3:26-33

16) Ehtesham M, Mapara KY, Stevenson CB, Thompson RC (2009) CXCR4 mediates the proliferation of glioblastoma progenitor cells. Cancer Lett 274:305-312

17) Hattermann K, Held-Feindt J, Lucius R, Müerköster SS, Penfold ME, Schall TJ, Mentlein R (2010) The chemokine receptor CXCR7 is highly expressed in human glioma cells and mediates antiapoptotic effects. Cancer Res 70:3299-3308.

18) Teicher BA, Fricker SP (2010) CXCL12 (SDF-1)/CXCR4 pathway in cancer. Clin Cancer Res. 16: 2927-2931

19) Redjal N, Chan JA, Segal RA, Kung AL (2006) CXCR4 inhibition synergizes with cytotoxic chemotherapy in gliomas. Clin Cancer Res 12:6765-6771

20) Hattermann K, Mentlein R. (2013) An Infernal Trio: The chemokine CXCL12 and its receptors CXCR4 and CXCR7 in tumor biology. Ann Anat 195:103-110

21) Ehtesham M, Winston JA, Kabos P, Thompson RC (2006) CXCR4 expression mediates glioma cell invasiveness. Oncogene 25:2801-2806

22) Osuka S, Sampetrean O, Shimizu T, Saga I, Onishi N, Sugihara E, Okubo J, Fujita S, Takano S, Matsumura A, Saya H (2012) IGF1 receptor signaling regulates adaptive radioprotection in glioma stem cells. Stem Cells 31:627-640

23) Sampetrean O, Saga I, Nakanishi M, Sugihara E, Fukaya R, Onishi N, Osuka S, Akahata M, Kai K,

Sugimoto H, Hirao A, Saya H (2011) Invasion precedes tumor mass formation in a malignant brain tumor model of genetically modified neural stem cells. Neoplasia 13:784-791

24) Bajetto A, Barbieri F, Dorcaratto A, Barbero S, Daga A, Porcile C, Ravetti JL, Zona G, Spaziante R, Corte G, Schettini G, Florio T (2006) Expression of CXC chemokine receptors 1-5 and their ligands in human glioma tissues: role of CXCR4 and SDF1 in glioma cell proliferation and migration. Neurochem Int 49:423-432

25) Calabrese C, Poppleton H, Kocak M, Hogg TL, Fuller C, Hamner B, Oh EY, Gaber MW, Finklestein D, Allen M, Frank A, Bayazitov IT, Zakharenko SS, Gajjar A, Davidoff A, Gilbertson RJ (2007) A perivascular niche for brain tumor stem cells. Cancer Cell 11:69-82

26) Hattermann K, Held-Feindt J, Lucius R, Müerköster SS, Penfold ME, Schall TJ, Mentlein R (2010) The chemokine receptor CXCR7 is highly expressed in human glioma cells and mediates antiapoptotic effects. Cancer Res 70:3299-3308

27) Salmaggi A, Boiardi A, Gelati M, Russo A, Calatozzolo C, Ciusani E, Sciacca FL, Ottolina A, Parati EA, La Porta C, Alessandri G, Marras C, Croci D, De Rossi M (2006) Glioblastoma-derived tumorospheres identify a population of tumor stem-like cells with angiogenic potential and enhanced multidrug resistance phenotype. Glia 54: 850-860.

28) Bao S, Wu Q, Sathornsumetee S, Hao Y, Li Z, Hjelmeland AB, Shi Q, McLendon RE, Bigner DD, Rich JN (2006) Stem cell-like glioma cells promote tumor angiogenesis through vascular endothelial growth factor. Cancer Res 66:7843-7848

29) Saini V, Staren DM, Ziarek JJ, Nashaat ZN, Campbell EM, Volkman BF, Marchese A, Majetschak M (2011) The CXC chemokine receptor 4 ligands ubiquitin and stromal cell-derived factor-1α function through distinct receptor interactions. J Biol Chem.286: 33466-33477

Figures

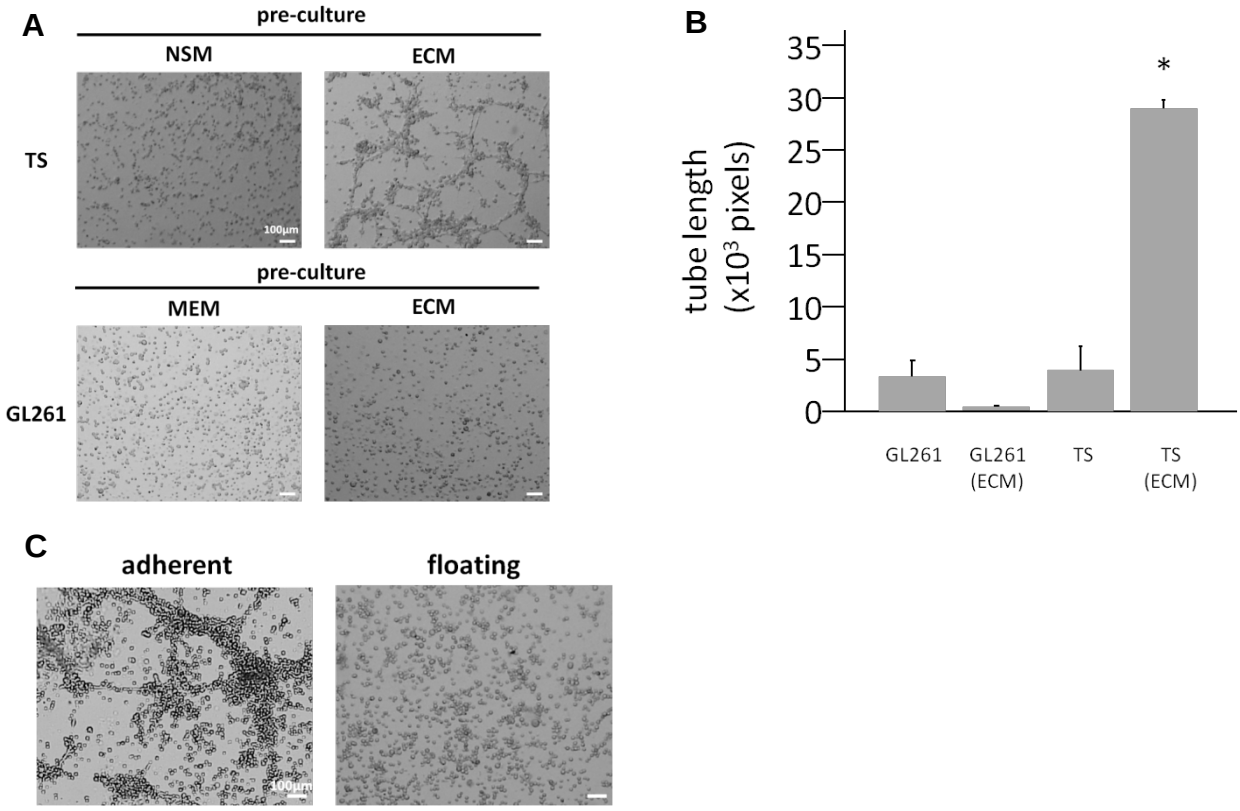

Fig. 1 In vitro culture of TS cells in endothelial conditions indicating functional features similar to endothelial cells.

A. Endothelial tube formation ability of TS cells and GL261 GBM cells. Tube formation was performed after pre-incubation for 10 days in neural stem cell medium (NSM), Minimal eagle medium (MEM), or endothelial cell medium (ECM). **B.** Mean tube lengths in the four groups (n = 3 per group) were assessed by counting four fields. *$p < 0.01$ compared to other cells (Tukey's HSD test). **C.** Endothelial tube formation ability by adherent TS cells and floating TS cells in ECM. Adherent-type TS cells formed tubes.

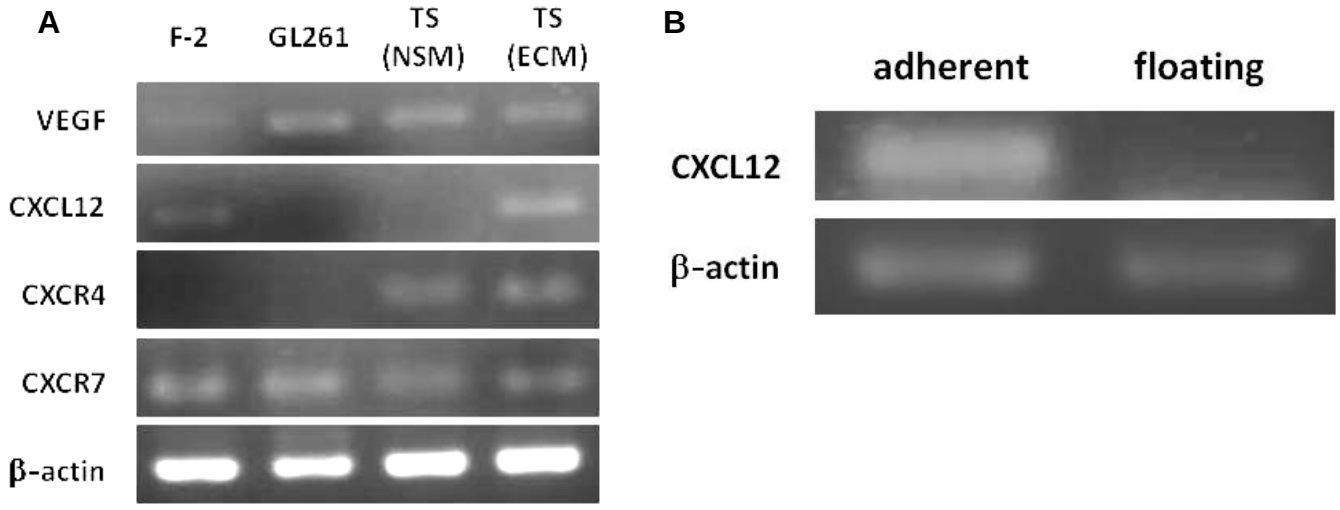

Fig. 2 In vitro culture of TS cells in endothelial conditions induces molecular features similar to endothelial cells.

A. The mRNA expression of VEGF, CXCL12, CXCR4, CXCR7, and β-actin in F-2 endothelial cells, GL261 GBM cells, and TS cells. TS cells were analyzed in neural stem cell medium (NSM) and endothelial cell medium (ECM). **B.** The mRNA expression of CXCL12 and β-actin in adherent TS cells and floating TS cells in ECM.

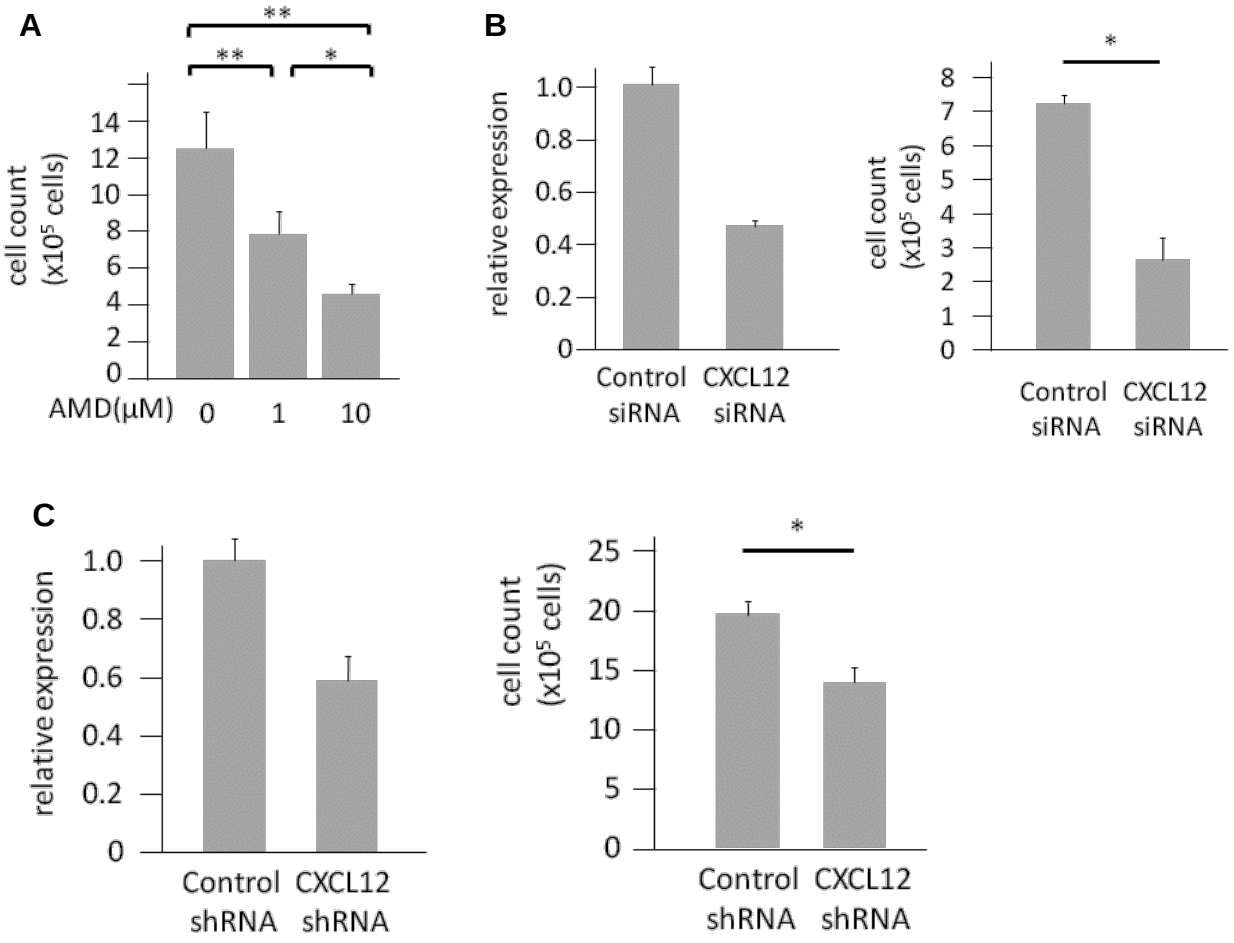

Fig. 3 The effect of blocking CXCL12/CXCR4 signaling on TS cell proliferation.

A. TS cell proliferation was examined when CXCL12/CXCR4 signaling was blocked using the CXCR4 antagonist, AMD3100. *$p < 0.05$, **$p < 0.01$, Tukey's HSD test. **B.** Left: Real-time RT-PCR analysis of the effect of siRNA targeting of CXCL12 on TS cells. Expression of CXCL12 mRNA was measured with quantitative real-time PCR and normalized to β-actin mRNA expression. Right: The effects of blocking CXCL12 signaling using CXCL12 siRNA in vitro. CXCL12 siRNA or control siRNA was transfected into 1×10^5 TS cells with Lipofectamine 2000. *$p < 0.01$ (Student's t-test). **C.** Left: Real-time RT-PCR analysis of the effect of shRNA targeting of CXCL12 in TS cells. Expression of CXCL12 mRNA was measured with quantitative real-time PCR and normalized to β-actin mRNA expression. Right: The effects of blocking CXCL12 signaling using CXCL12 shRNA in vitro. *$p < 0.01$ (Student's t-test).

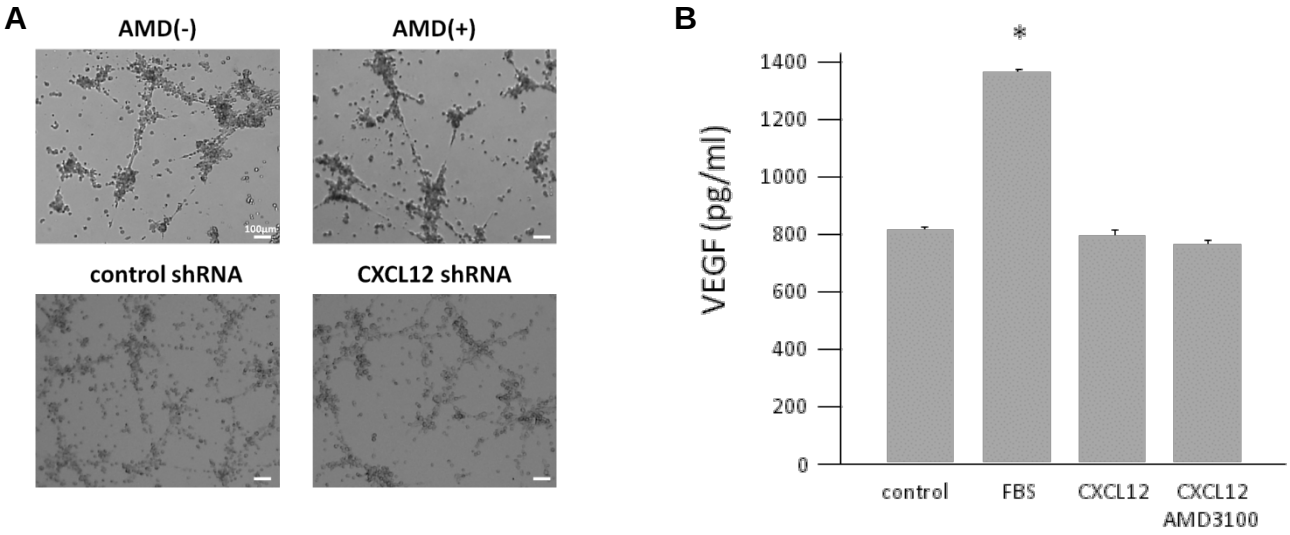

Fig. 4 Role of the CXCL12/CXCR4 pathway in endothelial cell-like changes.

A. Endothelial tube formation ability of TS cells. Tube formation was performed after pre-incubation in ECM for 10 days. AMD3100 was used at 10 μM during the pre-incubation. **B.** VEGF production by stimulated TS cells in culture medium. VEGF production (protein concentration; pg/ml) was determined with supernatants from TS cell cultures using ELISA. FBS was used at 2%; CXCL12 was used at 100 ng/ml; AMD3100 was used at 10 μM. Protein data are expressed as mean ± SEM. *$p < 0.01$, significant VEGF secretion was observed only in FBS treatment group, when compared to each other group (Tukey's HSD test).

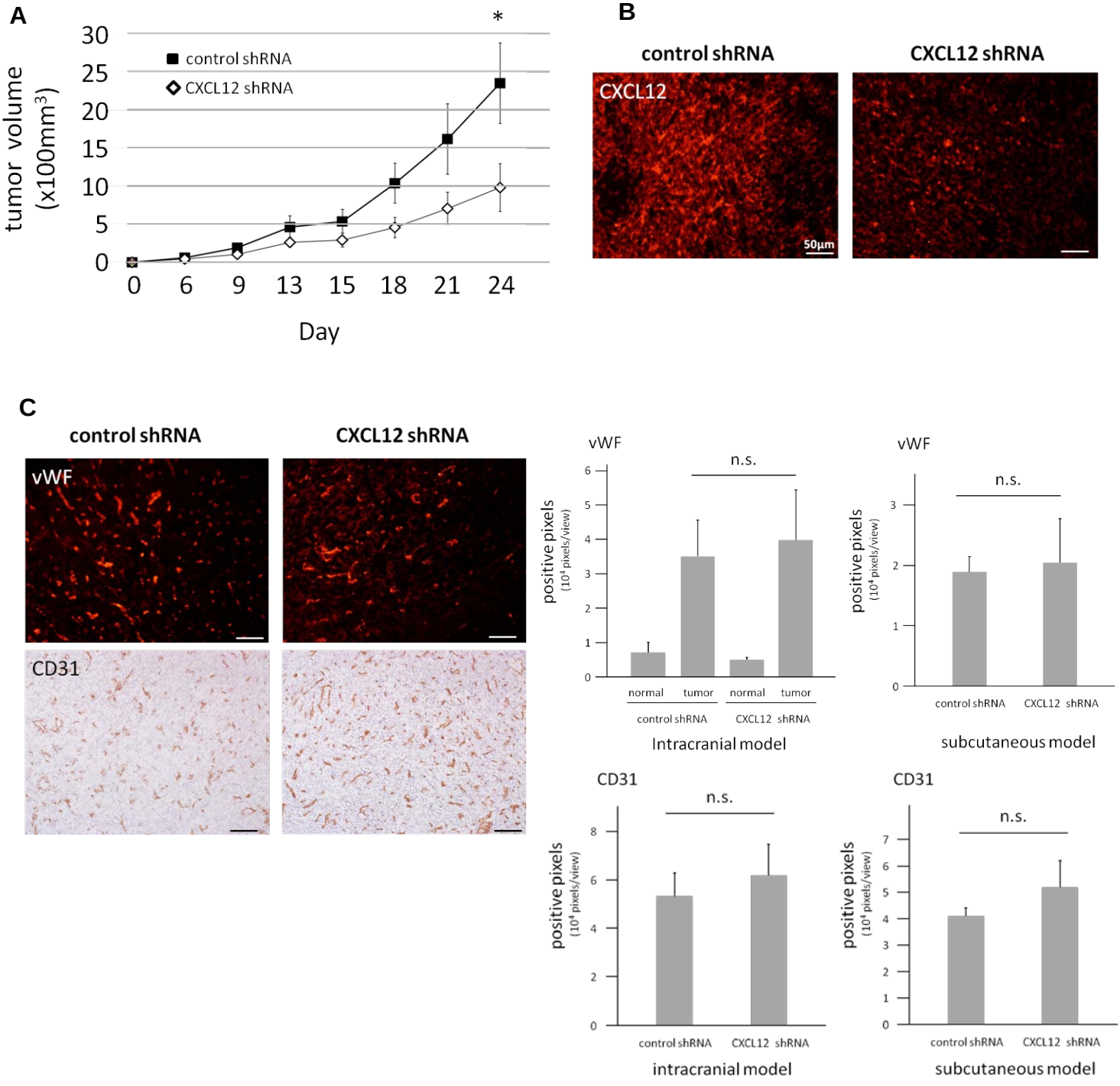
A
tumor volume (x100mm3)
control shRNA
CXCL12 shRNA
*
Day
B
control shRNA
CXCL12 shRNA
CXCL12
50μm
C
control shRNA
CXCL12 shRNA
vWF
CD31
vWF
positive pixels (10⁴ pixels/view)
n.s.
normal
tumor
normal
tumor
control shRNA
CXCL12 shRNA
Intracranial model
vWF
n.s.
positive pixels (10⁴ pixels/view)
control shRNA
CXCL12 shRNA
subcutaneous model
CD31
n.s.
positive pixels (10⁴ pixels/view)
control shRNA
CXCL12 shRNA
intracranial model
CD31
n.s.
positive pixels (10⁴ pixels/view)
control shRNA
CXCL12 shRNA
subcutaneous model

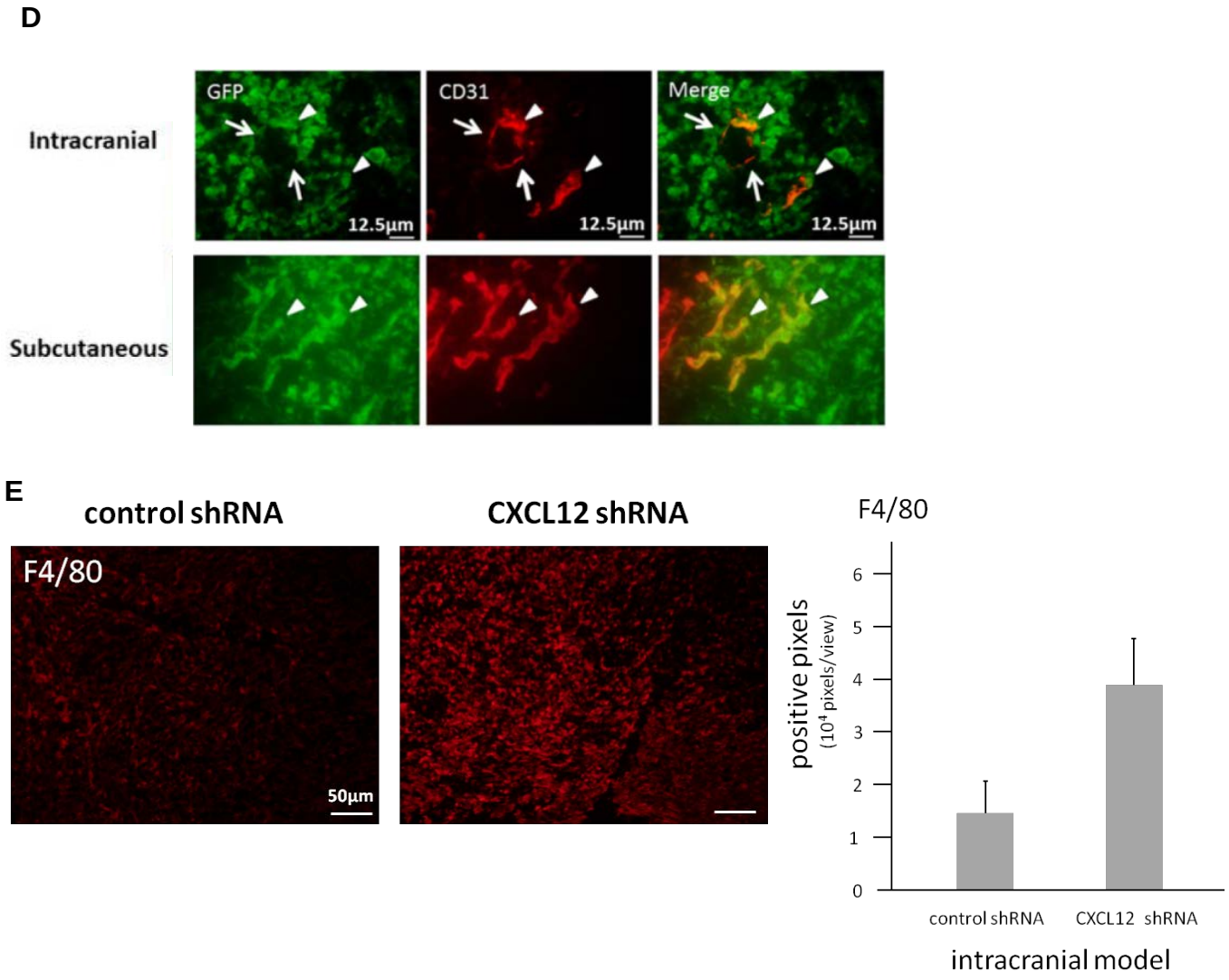

Fig. 5 Effect of blocking CXCL12 signaling in TS cells on tumor growth and angiogenesis.

A. The effect of blocking CXCL12/CXCR4 signaling using CXCL12 shRNA in an in vivo subcutaneous TS cell transplantation model. *$p < 0.05$ (Student's t-test). **B-E.** Immunohistochemical (IHC) analysis of CXCL12 (B), vWF (C), CD31 (C, D), and F4/80 (E). Comparison of positive areas in tumor tissue regions obtained from the TS cell transplantation model using IHC staining (intracranial tumor tissues obtained 2 weeks after implantation: control, n = 3, shRNA, n = 3; subcutaneous tumor tissues obtained 4.5 weeks after implantation: control, n = 3, shRNA, n = 5). Mean positive areas in the two groups were assessed by counting high-power fields with the most intense tumor site. CXCL12 is expressed in glioma tissues from TS cells. n.s. = not significant. Double staining for CD31 (red) and GFP (green) in the intracranial TS cell transplantation model (D, arrowhead, double-positive cell; arrow, CD31 single-positive cell).